Korean J. Chem. Eng., **31**(7), 1265-1270 (2014)
DOI: 10.1007/s11814-014-0045-z

pISSN: 0256-1115
eISSN: 1975-7220

Few-layered graphene oxides as superior adsorbents for the removal of Pb(II) ions from aqueous solutions

Wenbao Jia*,† and Songsheng Lu**

*Nanjing University of Aeronautics & Astronautics, 29 Yudao Street, Nanjing 210016, China
**New Star Institute of Applied Technology, No. 451 Huangshan Road, Hefei, Anhui 230031, China
(*Received 19 November 2013 • accepted 5 February 2014*)

Abstract−Few-layered graphene oxides (GOs) were successfully synthesized from graphite using Hummers' method. The synthesized GOs were characterized in detail by SEM, AFM, XRD, and FTIR spectroscopy. The prepared GOs were used as adsorbents to preconcentrate Pb(II) ions from large volumes of aqueous solutions. The effects of pH, ionic strength and temperature on the removal of Pb(II) ions from solution to GOs were investigated. The sorption of Pb(II) on GOs was dependent on pH values and independent of ionic strength, which suggested that Pb(II) sorption on GOs was mainly dominated by strong inner-sphere surface complexation. The maximum adsorption capacities (C_{smax}) of Pb(II) on GOs were calculated to be 344 mg/g at 293 K, 487 mg/g at 308 K, and 758 mg/g at 333 K, respectively. The C_{smax} values are the highest sorption capacities of today's materials for the sorption of Pb(II) ions from aqueous solutions. The thermodynamic parameters were calculated from the temperature-dependent sorption isotherms, and the results indicated that Pb(II) sorption on GOs was spontaneous and endothermic. The results suggested that the GOs were promising materials for the preconcentration of Pb(II) and other kinds of heavy metal ions from aqueous solutions in environmental pollution cleanup in real work.

Keywords: Graphene Oxides, Pb(II) Ions, Sorption, Thermodynamic Parameter, Interaction Mechanism

INTRODUCTION

Water pollution by different kinds of heavy metal ions is a crucial worldwide environmental pollution problem. Among the pollutants, lead is toxic for living species even at very low concentrations. Long-term consumption of water at high lead level will cause anemia, chills, diarrhea, headache and poisoning, leading to the dysfunction of kidneys, brain, liver and central nervous system [1-4]. Thereby, the elimination of Pb(II) from drinking water is crucial for the environmental pollution cleanup. In the last decade, various methods such as ion exchange, metal precipitation, metal ion extraction, chemical precipitation or coprecipitation, filtration, in-situ reduction/precipitation and sorption/adsorption, have been developed for the removal of heavy metal ions from large volumes of aqueous solutions [5-12]. Among these, sorption is considered as effective with the advantages of high treatment efficiency, easy operation, environmental friendliness, and can be used in large scale in real application. Many clay minerals and manmade nanomaterials have been applied as adsorbents to remove heavy metal ions from wastewater [13-17]. However, the low sorption ability of these materials restricted the application of these materials in real applications. Thereby, it is still a challenge to find new materials with high sorption capacities for the preconcentration of heavy metal ions in environmental pollution management.

Graphene oxides are a new kind of carbon nanomaterial with two-dimensional (2D) structure, the thickness determined by one or several atomic layers and the lateral sheets extending to up to several micrometers [18]. It consists of a hexagonal network of covalently linked carbon atoms with oxygen-containing functional groups attached to various sites, and has a very high aspect ratio and nominal surface area [19,20]. Because of the outstanding properties, numerous studies have been carried out on the electronic property [21], self-assembly [22] and its composites with other kinds of nanomaterials [23-25]. The preparation of graphene oxides from graphite using the Hummers method can introduce many oxygen-containing functional groups such as -COOH, -C=O-, and -OH groups on the surfaces of graphene oxides [26]. These oxygen-containing functional groups are important and essential for the binding of heavy metal ions, and thereby result in the high sorption capacity of graphene oxides. Graphene oxides are also hydrophilic and are easily dispersed in water to form stable colloidal suspensions, which makes them enhance adsorption ability through the formation of strong surface complexes with heavy metal ions or with organic pollutants through the π-π interactions etc. The sorption of organic and inorganic pollutants of graphene oxides has been studied extensively in the last several years [27-31], and the results suggest that the graphene oxides are favorable for the sorption of inorganic pollutants and the reduced graphene oxides are favorable for the sorption of organic pollutants [29,32-34]. Although the sorption of many kinds of organic pollutants and heavy metal ions on graphene oxides has been studied extensively, the sorption of Pb(II) on graphene oxides is still scarce [28,35].

In this paper, we report the synthesis of few-layered graphene oxides (GOs) from graphite, and the synthesized GOs were used as adsorbent to remove Pb(II) ions from aqueous solutions under different experimental conditions. The interaction mechanism of Pb(II) with GOs is discussed and the results demonstrate that the GOs have high sorption ability in the removal of Pb(II) ions from aqueous

†To whom correspondence should be addressed.
E-mail: jiawb422@163.com, jiawb@nuaa.edu.cn

solutions, which is very important for the application of GOs in environmental pollution management in real applications if graphene oxide can be synthesized at low price in large scale in near future.

EXPERIMENTS

1. Synthesis of Graphene Oxides

Graphene oxides were synthesized by using modified Hummers method [36,37] from the flake graphite (99.95% purity, Qingdao Tianhe Graphite Company, China). Briefly, 4.0 g graphite and 3.0 g of $NaNO_3$ were placed in a flask, and 300 mL H_2SO_4 was added with stirring in an ice-water bath. Then 18.0 g $KMnO_4$ was added slowly over about two hours. The stirring was continued for two hours in the ice-water bath and stirred for five days at 20±1 ºC, and then 560 mL 5 wt% H_2SO_4 was added over about 1 h with continuous stirring, and the temperature was kept at 98 ºC for 2 hours. After the temperature was reduced to 60 ºC, 12.0 mL H_2O_2 (30 wt%) was added, and the mixture was stirred for two hours at 20±1 ºC. The solid was separated from the suspension by centrifugation at 18,000 rpm, and then the solid was redispersed using vigorous stirring and bath ultrasonication for 30 min at the power of 140 W. The centrifugation and ultrasonication were recycled for several times, and finally the sample was rinsed with Milli-Q water until the solution was neutral. Thus achieved GOs products were dried in a vacuum tank at room temperature, and then stored in Milli-Q water to make its high dispersion in aqueous solutions and used in the following experiments.

2. Characterization of Graphene Oxides

Morphologies and sizes of the as-synthesized GOs were characterized by field emission scanning electron microscopy (FE-SEM) (JEOL JSM-6330F) at the beam energy of 15.0 kV, and by the Atomic Force Microscope (AFM) analysis, which was obtained in air using a Digital Instrumental Nanoscope III in tapping mode. The X-ray diffraction (XRD) pattern was measured on a D/max2500 with a Cu Kα source (λ=1.541 Å), and Fourier transformed infrared (FT-IR) spectroscopy was obtained by using a Nicolet Magana-IR 750 spectrometer over a range from 500 to 2,000 cm^{-1}.

3. Batch Sorption Experiments

The Pb(II) stock solution was prepared by using lead nitrate. The batch experiments of Pb(II) sorption from aqueous solution to GOs were carried out in polyethylene test tubes. Different amounts of the stock solution of GOs, $NaClO_4$ and Pb(II) solutions were added into the polyethylene test tubes to achieve the desired concentrations of different components. The pH values of the systems in each polyethylene test tube were adjusted by adding 0.01 mol/L NaOH or $HClO_4$ solutions. The polyethylene test tubes were shaken for 24 h to achieve sorption equilibrium, then the solid phase was separated from the solution by centrifugation at 18,000 rpm for 30 minutes and the supernatant was filtrated using 0.22 μm membrane filters. The concentration of Pb(II) in filtrate was determined by spectrophotometry at the wavelength of 616 nm using Pb(II)-Chlorophosphonazo(III) complex [38,39]. All the experiments were carried out in duplicate, and the relative errors were about 5%. The amounts of Pb(II) adsorbed on GOs were calculated from the difference between the initial concentration (C_0) and the equilibrium one (C_e):

$$\text{Adsorption}\% = (C_0 - C_e)/C_0 \times 100\% \quad (1)$$

$$C_s = (C_0 - C_e)/m_{adsorbent} \times V \quad (2)$$

where C_s is the amount of Pb(II) adsorbed on GOs, V is the volume of the suspension, and $m_{adsorbent}$ is the mass of GOs in the suspension.

RESULTS AND DISCUSSION

1. Characterization of GOs

From the SEM image (Fig. 1(a)) one can see that few-layered graphene oxide nanosheets were formed. The synthesized GOs have lateral dimensions of several micrometers with the small holes caused by the overexposure to sonication. From the AFM image (Fig. 1(b)),

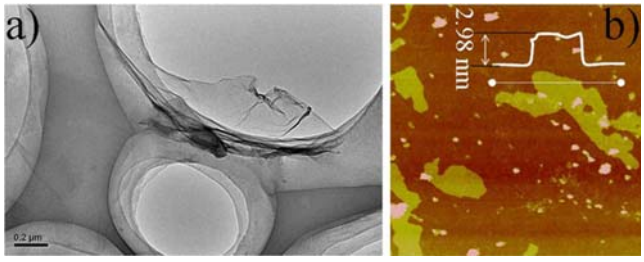

Fig. 1. SEM image (a) and AFM image (b) of GOs on Si/SiO_2 substrates (SiO_2 ca. 300 nm).

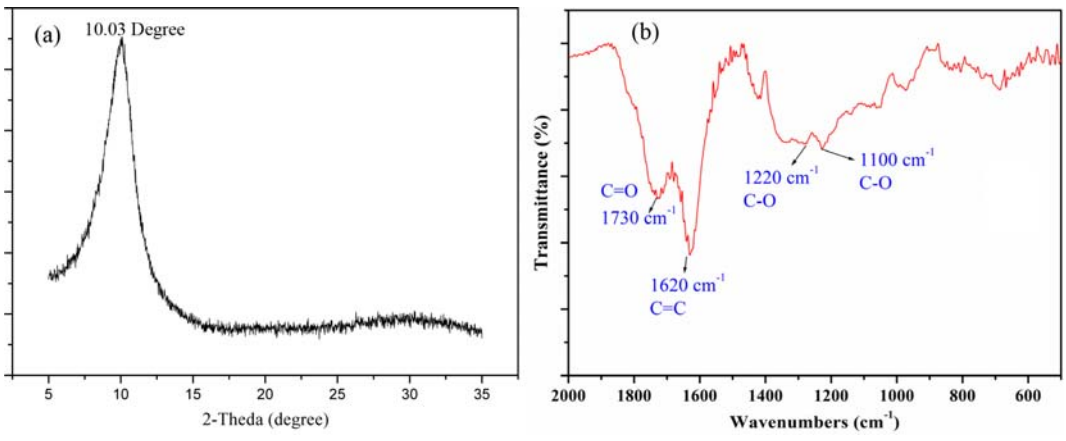

Fig. 2. XRD pattern (a) and FTIR spectrum (b) of GOs.

the thickness of the GO nanosheets was about 2.98 nm, suggesting that few-layered GO nanosheets were synthesized [40,41]. The thickness of one layer graphene oxide nanosheet was ~0.8-1.0 nm [40]. The layer thickness of the GO sample on Si/SiO_2 substrates suggested that 2 or 3-layered graphene oxide nanosheets were formed.

The XRD pattern of GOs is shown in Fig. 2(a). The broad and relatively weak diffraction peak at 2θ=10.03° with d=0.87 nm corresponds to the typical diffraction peak of GOs, which was attributed to the (002) plane. It is well known that the c-axis spacing of graphite is 0.34 nm, and the c-axis spacing increased from 0.34 nm to 0.87 nm after the graphite was modified to graphene oxide nanosheets during the oxidation processes, which was due to the creation of the oxygen-containing functional groups on the surfaces of GO [42-44]. The oxygen-containing functional groups were evidenced by the following FTIR analysis.

The oxygen-containing functional groups on the surfaces of GO nanosheets were characterized by FT-IR analysis (Fig. 2(b)). One can see that different functional groups were found in the FTIR spectrum, such as -C-O- group at 1,100 cm^{-1} and 1,220 cm^{-1}, -C=C group at 1,620 cm^{-1} and -C=O group at 1,730 cm^{-1}. These peaks suggest that large amounts of oxygen-containing functional groups existed on the surfaces of GO nanosheets [45].

2. Effect of pH and Ionic Strength on Pb(II) Sorption onto Graphene Oxides

The sorption of Pb(II) ions on GOs in 0.001 M and 0.01 M $NaClO_4$ solutions at different pH values is shown in Fig. 3. One can see that that the sorption of Pb(II) on GOs increased with pH increasing from 2.5 to 5.5, maintained the high level at pH 5.5 to 7.5, and then decreased with increasing pH values at pH>7.5. The sorption of Pb(II) on GOs increased slowly with pH increasing at pH<4, and sharply with pH increasing in the pH range of 4 to 5.5. The pH_{pzc} (point of zero charge) value of GOs was calculated to be 3.89 from the acid-base titration curves [30]. At pH<pH_{pzc}, the surface charge was positive, while at pH>pH_{pzc}, the surface charge was negative. At pH<4, the sorption of Pb(II) ions on the positively charged surface of GOs was mainly attributed to ion exchange of Pb^{2+} ions with Na^+/H^+ ions on GO surfaces. From the characterization results, the following assumptions were made to account for Pb(II) sorption on GOs: (1) the sorption sites were assumed to be carboxyl and hydroxyl groups; (2) the GO nanosheets behave like a collection of simple ligands and there were no interactions between the two different binding sites; and (3) two kinds of intrinsic acidity constants were used to model the surface complexation of the carboxyl and hydroxyl groups with Pb(II) ions [46,47]. The surface protonation and deprotonation reactions can be expressed as follows:

$$\equiv SOH + H^+_{(s)} \Leftrightarrow \equiv SOH^+_2 \quad (3)$$

$$\equiv SOH \Leftrightarrow \equiv SO^- + H^+_{(s)} \quad (4)$$

$$\equiv XOH + H^+_{(s)} \Leftrightarrow \equiv XOH^+_2 \quad (5)$$

$$\equiv XOH \Leftrightarrow \equiv XO^- + H^+_{(s)} \quad (6)$$

where, $\equiv SOH$, $\equiv SOH^+_2$ and $\equiv SO^-$ represent the neutral, positively charged, and negatively charged carboxyl groups on GO surface, respectively. Whereas $\equiv XOH$, $\equiv XOH^+_2$ and $\equiv XO^-$ represent the neutral, positively charged, and negatively charged hydroxyl groups on GO surface, respectively. $H^+_{(s)}$ is the proton concentration on the surface of GO nanosheets. From the hydrolysis constants of Pb(II) ions [48], Pb(II) ions present in the species of Pb^{2+}, $Pb(OH)^+$, $Pb(OH)^0_2$, $Pb(OH)^-_3$ at different pH values (Fig. 4). The main species of Pb(II) ions are Pb^{2+} and $Pb(OH)^+$ at low pH values. While at high pH values, the predominant Pb(II) species is $Pb(OH)^-_3$, which is difficult to be adsorbed on the negative charged surface of GOs due to the electrostatic repulsion. At high pH values, the functional groups of GOs are progressively deprotonated to form negative surface charge, and thereby the negatively charged Pb(II) species are difficult to be adsorbed on the negatively charged GOs [49].

From Fig. 3, the sorption of Pb(II) ions on GOs was not affected by the concentrations of $NaClO_4$ under the experimental conditions. The ionic strength-independent and pH-dependent sorption results suggest that the sorption of Pb(II) from aqueous solutions to GOs was mainly dominated by strong inner-sphere surface complexation rather than by outer-sphere surface complexation [50,51]. From the precipitation constant of $Pb(OH)_2$(s) (1.2×10^{-15}) [28], it is evident that Pb(II) ions did not form precipitates on GO surfaces and the

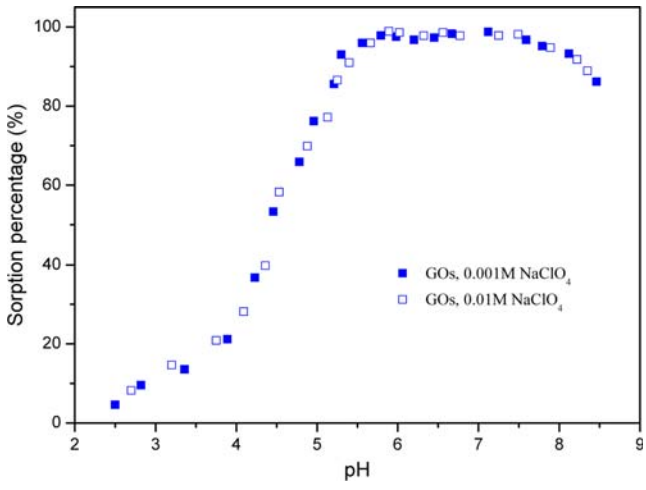

Fig. 3. The effect of pH and ionic strength on Pb(II) adsorption onto GOs. T=293±1 K, $C[Pb^{2+}]_{(initial)}$=100.0 mg/L, m/V=0.25 g/L.

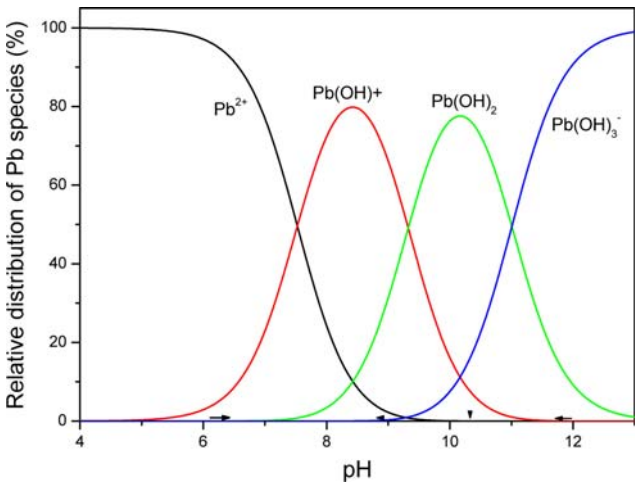

Fig. 4. Relative distribution of Pb(II) species in 0.01 M $NaClO_4$ solution as a function of pH based on the equilibrium constants.

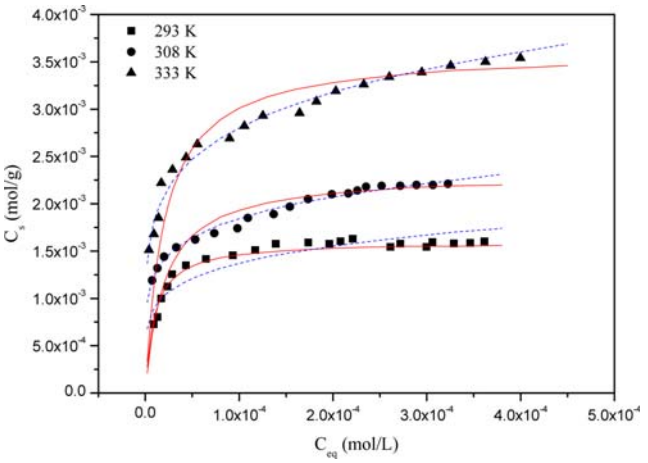

Fig. 5. Adsorption isotherms of Pb(II) on GOs at three temperatures. pH=5.8±0.1, C[$NaClO_4$]=0.01 mol/L, m/V=0.25 g/L. Solid lines: Langmuir model simulation; FGO; Dashed lines: Freundlich model simulation.

contribution of Pb(II) precipitation on Pb(II) sorption to GOs was negligible. More than 99% Pb(II) ions were adsorbed to GOs at pH 5.5, thereby it was impossible to form precipitates because of the very low concentration of free Pb(II) ions remaining in aqueous solutions. The high sorption of Pb(II) on GOs is mainly attributed to the strong surface complexation of Pb(II) with the functional groups on GO surfaces [52].

3. Adsorption Isotherms and Thermodynamic Parameters

The Pb(II) sorption isotherms GOs at T=293, 308, and 333 K are shown in Fig. 5. One can see that the sorption isotherm of Pb(II) on GOs was the highest at the temperature of 333 K and was the lowest at the temperature of 293 K. The results suggest that the sorption of Pb(II) on GOs was promoted at higher temperature, and the sorption of Pb(II) was an endothermic process. To simulate the sorption data of Pb(II) on GOs, we applied the Langmuir isotherm model and Freundlich isotherm model to simulate the sorption data of Pb(II) on GOs at different temperatures. The Langmuir model was applied to describe the sorption isotherms of heavy metal ions on solid particles, which assumed that (1) the sorption was limited on monolayer coverage of solid particles,(2) all sorption sites were alike, and (3) the sorption ability of the metal ions on the given site was independent of its neighboring sites occupancy [53,54]. The Langmuir isotherm model was expressed as:

$$\frac{C_e}{C_s}=\frac{1}{K_L C_{s\,max}}+\frac{C_e}{C_{s\,max}} \tag{7}$$

where C_e is the equilibrium concentration of Pb(II) in aqueous solution, C_s is the amount of Pb(II) adsorbed on per weight of GOs, C_{smax} is the maximum adsorbed amount of Pb(II) on per weight of GOs, which is a complete monolayer coverage on the surface of GOs at high Pb(II) concentrations, and K_L represents the enthalpy of sorption.

The Freundlich isotherm model is a semi-empirical equation which describes the sorption of metal ions on heterogeneous surface of solid particles and it is usually expressed as [55]:

$$C_s=K_F C_e^n \tag{8}$$

Eq. (8) can be expressed in linear form as:

Table 1. The parameters for Pb(II) sorption on GOs at different temperatures

Correlation parameters		T=293 K	T=308 K	T=333 K
Langmuir	$C_{s\,max}$ (mol·g^{-1})	1.64×10^{-3}	2.32×10^{-3}	3.61×10^{-3}
	b (L·mol^{-1})	1.04×10^{5}	5.00×10^{4}	5.04×10^{4}
	R^2	0.999	0.998	0.998
Freundlich	k_F (mol^{1-n}·L^n·g^{-1})	7.19×10^{-3}	8.59×10^{-3}	1.51×10^{-2}
	n	0.18	0.17	0.18
	R^2	0.918	0.994	0.988

$$\log C_s=\log K_F+n\log C_e \tag{9}$$

where k_F (mol^{1-n}L^n/g) represents the sorption capacity at metal ion equilibrium concentration equaling to 1, and n represents the degree of sorption dependence with sorption equilibration.

The Langmuir and Freundlich isotherm parameters simulated from the sorption isotherms are listed in Table 1. From the R^2 values, the Langmuir model simulated the sorption isotherms better than did the Freundlich model. The maximum sorption capacities (C_{smax}) of Pb(II) ions on GOs at 293, 308, and 333 K were 1.64×10^{-3}, 2.32×10^{-3}, and 3.61×10^{-3} mol/g, respectively. The sorption of Pb(II) on GOs increased with increasing temperature. The sorption capacity of GOs is an important parameter to evaluate its application in the elimination of heavy metal ions from aqueous solution in real applications. Compared to other kinds of materials, the C_{smax} values of Pb(II) sorption on GOs were much higher than those of Pb(II) sorption on other materials (Table 2). One can see that the GOs had the highest sorption capacity towards Pb(II) ions from aqueous solutions, which may be attributed to the main oxygen-containing functional groups (i.e., C-O and C=O groups) on the surfaces of GOs. From the result of XRD analysis (Fig. 2(a)), the c-axis spacing of GO is 0.87 nm, which is enough for the Pb^{2+} ions (r ~0.48 nm) to enter into the interlayer space of GO. This also contributes to Pb^{2+} sorption on GO. The abundant oxygen-containing functional groups on the surfaces of GOs made the 2 or 3 adjacent oxygen atoms available to form complexes with Pb(II) ions on the surface of GOs. The strong interaction between Pb(II) and functional groups of GOs is responsible for the high-efficiency sorption of Pb(II) ions on GOs.

The thermodynamic data (i.e., ΔH^0, ΔS^0, and ΔG^0) for Pb(II) sorption on GOs were obtained from the temperature-dependent sorption isotherms. The values of standard entropy change (ΔS^0) and standard enthalpy change (ΔH^0) were calculated from the y-intercept

Table 2. Maximum adsorption capacity of Pb(II) onto various adsorbents

Adsorbents	C_{smax} (mg/g)	Conditions	References
Activated carbon	21.80	pH 6.0, T 303 K	[58]
Iron oxide	36.00	pH 5.5, T 298 K	[59]
GMZ Bentonite	23.83	pH 5.2, T 293 K	[61]
Hazelnut shell	28.18	pH 6.0, T 298 K	[60]
Oxidized MWCNTs	2.06	pH 6.0, T 293 K	[2]
Graphene nanosheets	22.42	pH 4.0, T 303 K	[35]
Graphene oxides	344	pH 5.8, T 293 K	This work
Reduced graphene oxide	500	pH 6.0, T 298 K	[62]

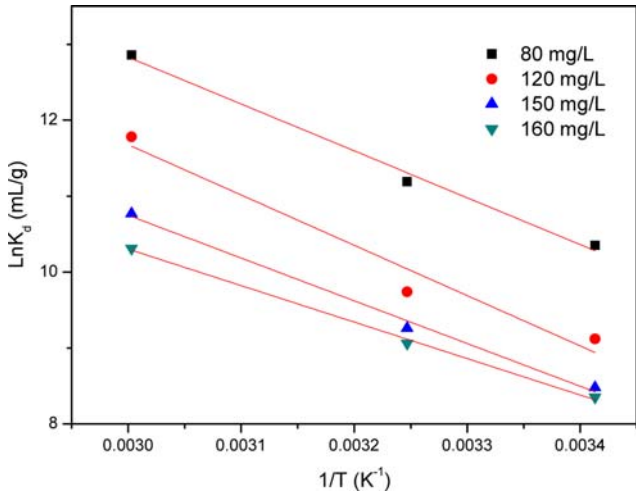

Fig. 6. Linear plots of LnK_d vs. 1/T for the sorption of Pb(II) on GOs at 293, 308, 333 K. pH=5.8±0.1, C[$NaClO_4$]=0.01 mol/L, m/V=0.25 g/L.

Table 3. Thermodynamic parameters for Pb(II) sorption on GOs

C_0	ΔH^0	ΔS^0	ΔG^0 (kJ·mol^{-1})		
(mol·L^{-1})	(kJ·mol^{-1})	(J·mol^{-1}·K^{-1})	293 K	308 K	333 K
3.81×10^{-4}	55.09	262.3	–21.68	–25.61	–32.16
5.71×10^{-4}	51.30	260.7	–25.17	–29.09	–35.61
7.14×10^{-4}	46.81	222.3	–18.24	–21.57	–27.12
7.61×10^{-4}	39.91	205.4	–20.15	–23.23	–28.36

and slope of the plot of $\ln K_d$ vs. 1/T (Fig. 6) by using the following equation:

$$\ln K_d = \frac{\Delta S^0}{R} - \frac{\Delta H^0}{RT} \quad (10)$$

The Gibbs free energy changes (ΔG^0) were calculated from the following equation:

$$\Delta G^0 = \Delta H^0 - T\Delta S^0 \quad (11)$$

Relevant thermodynamic parameters calculated from Eqs. (10) and (11) are tabulated in Table 3. From the values listed there, one can see that the ΔH^0 values were positive, suggesting that the sorption of Pb(II) on GOs is an endothermic process. The interpretation of the endothermicity of enthalpy of Pb(II) sorption was that the free Pb(II) ions were well solvated in aqueous solutions. To adsorb on GOs, these ions were to some extent denuded the hydration sheath, and this dehydration process needed energy. This energy of dehydration exceeded the exothermicity of the Pb(II) ions attaching to GO surfaces. Because the removal of water molecules from Pb(II) ions is an endothermic process, the endothermicity of the desolvation process exceeded that of the enthalpy of sorption to a considerable extent. The Gibbs free energy changes (ΔG^0) were negative as expected for the spontaneous process under the experimental conditions. The decrease of ΔG^0 with temperature increasing indicated that the sorption of Pb(II) ions on GOs was more efficient at higher temperature. At higher temperature, the Pb(II) ions were readily dehydrated, and the sorption became more favorable. The positive entropy change (ΔS^0) also indicated that the sorption process was spontaneous [56,57].

CONCLUSIONS

We synthesized few-layered graphene oxides with high oxygen-containing functional groups from graphite by using the Hummers method. The synthesized graphene oxides were applied as adsorbents to preconcentrate Pb(II) ions from aqueous solutions, and the results suggested that the sorption of Pb(II) on GOs was strongly dependent on pH and independent of ionic strength. The thermodynamic parameters calculated from the temperature-dependent sorption isotherms indicated that the sorption of Pb(II) on GOs was endothermic and spontaneous. The GOs had the highest sorption capacity of today's materials. Because of the strong surface complexation of the oxygen-containing groups with metal ions, we can conclude that the GOs would be a promising material for the preconcentration and solidification of heavy metal ions in the heavy metal ion pollution cleanup in real work if graphene oxides could be synthesized in large scale and at low price in near future. It is a little difficult to separate GO from aqueous solutions in large scale. However, if some magnetic particles are deposited on GO surface, then the GO magnetic nanocomposites could be separated from aqueous solution using magnetic separation method in large scale. Considering the high sorption capacity of GO and easy magnetic separation method, the GO magnetic nanocomposites could be used in large scale applications. The simultaneous elimination of organic and inorganic pollutants from aqueous solutions by using the graphene oxides or GO magnetic nanocomposites should be carried out in the future to evaluate the possible application of graphene oxides in wastewater treatment.

ACKNOWLEDGEMENT

Financial support from National Natural Science Foundation of China (21375148) is acknowledged.

REFERENCES

1. C. K. Singh, J. N. Sahu, K. K. Mahalik, C. R. Mohanty, B. R. Mohan and B. C. Meikap, *J. Hazard. Mater.*, **153**, 221 (2008).
2. D. Xu, X. L. Tan, C. L. Chen and X. K. Wang, *J. Hazard. Mater.*, **154**, 407 (2008).
3. D. Xu, X. L. Tan, C. L. Chen and X. K. Wang, *Appl. Clay Sci.*, **41**, 37 (2008).
4. X. Tan, P. Chang, Q. Fan, X. Zhou, S. Yu, W. Wu and X. Wang, *Colloids Surf., A.*, **328**, 8 (2008).
5. J. F. Li, Y. M. Li and J. H. Lu, *Appl. Clay Sci.*, **46**, 314 (2009).
6. Y. Zhang, Y. Li and X. Zheng, *Sci. Total Environ.*, **409**, 625 (2011).
7. G. D. Sheng, S. W. Wang, J. Hu, Y. Lu, J. X. Li, Y. H. Dong and X. K. Wang, *Colloids Surf., A.*, **339**, 159 (2009).
8. J. Hu, D. D. Shao, C. L. Chen, G. D. Sheng, J. X. Li, X. K. Wang and M. Nagatsu, *J. Phys. Chem. B*, **114**, 6779 (2010).
9. J. Li, M. Jiang, H. Wu and Y. Li, *J. Agric. Food Chem.*, **56**, 1336 (2009).
10. D. Shao, Z. Jiang and X. Wang, *Plasma Process Polym.*, **7**, 552 (2010).

11. J. Li, Y. Li and H. Dong, *J. Agric. Food Chem.*, **56**, 1336 (2008).
12. Q. H. Fan, X. L. Tan, J. X. Li, X. K. Wang, W. S. Wu and G. Montavon, *Environ. Sci. Technol.*, **43**, 5776 (2009).
13. Y. Zhang, Y. Li, J. Li, G. Sheng, Y. Zhang and X. Zheng, *Chem. Eng. J.*, **185-186**, 243 (2012).
14. C. Chen, X. Wang and M. Nagatsu, *Environ. Sci. Technol.*, **43**, 2362 (2009).
15. D. Shao, J. Hu and X. Wang, *Plasma Process Polym.*, **7**, 977 (2010).
16. S. Yang, J. Hu, C. Chen, D. Shao and X. Wang, *Environ. Sci. Technol.*, **45**, 3621 (2011).
17. Y. Li, Y. Zhang, J. Li and X. Zheng, *Environ. Pollut*., **159**, 3744 (2011).
18. G. Zhao, T. Wen, C. Chen and X. Wang, *RSC Adv.*, **2**, 9286 (2012).
19. J. Li, S. Zhang, C. Chen, X. Yang, J. Li and X. Wang, *ACS Appl. Mater. Interf.*, **4**, 4991 (2012).
20. Y. B. Sun, Q. Wang, C. L. Chen, X. L. Tan and X. K. Wang, *Environ. Sci. Technol.*, **46**, 6020 (2012).
21. V. C. Tung, M. J. Allen, Y. Yang and R. B. Kaner, *Nature Nano*, **4**, 25 (2009).
22. J. M. Mativetsky, E. Treossi, E. Orgiu, M. Melucci, G. P. Veronese, P. Samorì and V. Palermo, *J. Am. Chem. Soc.*, **132**, 14130 (2010).
23. D. Zhao, G. Sheng, C. Chen and X. Wang, *Appl. Catal. B: Environ.*, **111-112**, 303 (2012).
24. L. Tian, M. J. Meziani, F. Lu, C. Y. Kong, L. Cao, T. J. Thorne and Y. P. Sun, *ACS Appl. Mater. Interf.*, **2**, 3217 (2010).
25. L. Zhang, S. Zhao, X. Tian and X. Zhao, *Langmuir*, **26**, 17624 (2010).
26. G. Zhao, L. Jiang, Y. He, J. Li, H. Dong, X. Wang and W. Hu, *Adv. Mater.*, **23**, 3959 (2011).
27. Y. B. Sun, D. D. Shao, C. L. Chen, S. B. Yang and X. K. Wang, *Environ. Sci. Technol.*, **47**, 9904 (2013).
28. G. Zhao, X. Ren, X. Gao, X. Tan, J. Li, C. Chen, Y. Huang and X. Wang, *Dalton Trans.*, **40**, 10945 (2011).
29. X. Yang, C. Chen, J. Li, G. Zhao, X. Ren and X. Wang, *RSC Adv.*, **2**, 8821 (2012).
30. G. Zhao, T. Wen, X. Yang, S. Yang, J. Liao, J. Hu, D. Shao and X. Wang, *Dalton Trans.*, **41**, 6182 (2012).
31. Y. Sun, S. Yang, G. Zhao, Q. Wang and X. Wang, *Chem. Asian J.*, **8**, 2755 (2013).
32. X. M. Ren, C. L. Chen, M. Nagatsu and X. K. Wang, *Chem. Eng. J.*, **170**, 395 (2011).
33. K. Lv, G. Zhao and X. Wang, *Chinese Sci. Bull.*, **57**, 1223 (2012).
34. S. W. Zhang, M. Y. Zeng, W. Q. Xu, J. X. Li, J. Li, J. Z. Xu and X. K. Wang, *Dalton Trans.*, **42**, 7854 (2013).
35. Z. H. Huang, X. Y. Zeng, W. Lv, M. Wang, Q. H. Yang and F. Y. Kang, *Langmuir*, **27**, 7558 (2011).
36. M. Hirata, T. Gotou, S. Horiuchi, M. Fujiwara and M. Ohba, *Carbon*, **42**, 2929 (2004).
37. Q. Wang, X. Wang, Z. Chai and W. Hu, *Chem. Soc. Rev.*, **42**, 8821 (2013).
38. J. Li, S. Chen, G. Sheng, J. Hu, X. Tan and X. Wang, *Chem. Eng. J.*, **166**, 551 (2011).
39. X. Ren, D. Shao, S. Yang, J. Hu, G. Sheng, X. Tan and X. Wang, *Chem. Eng. J.*, **170**, 170 (2011).
40. L. Zhang, J. J. Liang, Y. Huang, Y. F. Ma, Y. Wang and Y. S. Chen, *Carbon*, **47**, 3365 (2009).
41. L. Zhang, X. Li, Y. Huang, Y. F. Ma, X. J. Wan and Y. S. Chen, *Carbon*, **48**, 2367 (2010).
42. X. Fan, W. Peng, Y. Li, X. Li, S. Wang, G. Zhang and F. Zhang, *Adv. Mater.*, **20**, 4490 (2008).
43. M. J. McAllister, J. L. Li, D. H. Adamson, H. C. Schniepp, A. A. Abdala, J. Liu, M. Herrera-Alonso, D. L. Milius, R. Car, R. K. Prud'homme and I. A. Aksay, *Chem. Mater.*, **19**, 4396 (2007).
44. X. Meng, D. Geng, J. Liu, M. N. Banis, Y. Zhang, R. Li and X. Sun, *J. Phys. Chem. C*, **114**, 18330 (2010).
45. G. Zhao, J. Li, X. Ren, C. Chen and X. Wang, *Environ. Sci. Technol.*, **45**, 10454 (2011).
46. C. L. Chen, J. Hu, D. Xu, X. L. Tan, Y. D. Meng and X. K. Wang, *J. Colloid Interface Sci*., **323**, 33 (2008).
47. D. A. Dzombak and F. M. M. Morel, *Surface complexation modeling, Hydrous ferric Oxide*, John Wiley and Sons Inc. New York (1990).
48. C. H. Weng, *J Colloid Interface Sci.*, **272**, 262 (2004).
49. S. T. Yang, G. D. Sheng, X. L. Tan, J. Hu, J. Z. Du, G. Montavon and X. K. Wang, *Geochim. Cosmochim. Acta*, **75**, 6520 (2011).
50. G. Sheng, S. Yang, J. Sheng, J. Hu, X. Tan and X. Wang, *Environ. Sci. Technol.*, **45**, 7718 (2011).
51. S. Yang, G. Sheng, G. Montavon, Z. Guo, X. Tan, B. Grambow and X. Wang, *Geochim Cosmochim Acta*, **121**, 84 (2013).
52. X. L. Tan, Q. H. Fan, X. K. Wang and B. Grambow, *Environ. Sci. Technol.*, **43**, 3115 (2009).
53. I. Langmuir, *J. Am. Chem. Soc.*, **40**, 1361 (1918).
54. S. Yang, P. Zong, X. Ren, Q. Wang and X. Wang, *ACS Appl. Mater. Interf.*, **4**, 6891 (2012).
55. Q. Wang, J. Li, Y. Song and X. Wang, *Chem. Asian J.*, **8**, 225 (2013).
56. T. Wen, X. Wu, X. Tan, Q. Zhu, A. Xu and X. Wang, *ACS Appl. Mater. Interf.*, **5**, 3304 (2013).
57. C. L. Chen and X. Wang, *Ind. Eng. Chem. Res.*, **45**, 9144 (2006).
58. M. M. Rao, D. K. Ramana, K. Seshaiah, M. C. Wang and S. W. C. Chien, *J. Hazard. Mater.*, **166**, 1006 (2009).
59. N. Nassar, *J. Hazard. Mater.*, **184**, 538 (2010).
60. E. Pehlivan, T. Altun, S. Cetin and M. Iqbal Bhanger, *J. Hazard. Mater.*, **167**, 1203 (2009).
61. S. Wang, Y. Dong, M. He, L. Chen and X.Yu, *Appl. Clay Sci.*, **43**, 164 (2009).
62. Y. F. Yang, Y. L. Xie, L. C. Pang, M. Li, X. H. Song, J. G. Wen and H. Y. Zhao, *Langmuir*, **29**, 10727 (2013).